Am J Transl Res 2016;8(9):3666-3677
www.ajtr.org /ISSN:1943-8141/AJTR0035015

*Original Article*

# Therapeutic ultrasound reverses peripheral ischemia in type 2 diabetic mice through PI3K-Akt-eNOS pathway

Zhao-Yang Lu[1,2*], Rui-Lin Li[1,2*], Hong-Sheng Zhou[3*], Jing-Juan Huang[4], Zhi-Xiao Su[1], Jia Qi[1], Lan Zhang[2], Yue Li[5], Yi-Qin Shi[6], Chang-Ning Hao[2], Jun-Li Duan[1]

*[1]Department of Gerontology, Xinhua Hospital, Shanghai Jiaotong University School of Medicine, Kongjiang Road 1665, Shanghai 200092, China; [2]Department of Vascular Surgery, Ren Ji Hospital, Shanghai Jiaotong University School of Medicine, Dongfang Road 1630, Shanghai 200127, China; [3]Shanghai Acoustics Laboratory, Chinese Academy of Science, Xiaomuqiao Road 456, Shanghai 200032, China; [4]Department of Cardiology, Shanghai Chest Hospital, Shanghai Jiaotong University, Huaihai Xi Road 241, Xuhui District, Shanghai 200030, China; [5]Department of Internal Medicine, University of Iowa Carve College of Medicine 2000 Medical laboratories, 25 South Grand Avenue, Iowa City, IA 52242, USA; [6]Department of Nephrology Zhongshan Hospital, Fudan University, Fenglin Road 180, Shanghai 200032, China. [*]Equal contributors.*

Received July 4, 2016; Accepted September 1, 2016; Epub September 15, 2016; Published September 30, 2016

**Abstract:** Therapeutic ultrasound (TUS) has been demonstrated to improve endothelial nitric oxide synthase (eNOS) activity, which played a crucial role in the regulation of angiogenesis. Diabetes Mellitus (DM) impairs eNOS activity. We tested the hypothesis that DM may retard unilateral hindlimb ischemia-induced angiogenesis by inhibiting eNOS in high-fat diet (HFD)/streptozocin (STZ) induced diabetic mice, and that TUS may reverse DM-related impairment of angiogenesis. C57BL/6 mice were allocated to four groups: (A) mice were fed standard diet (control); (B) mice were fed standard diet and treated with TUS (control+TUS); (C) type-2 DM mice were induced by HFD/STZ (diabetic); and (D) type-2 DM mice and treated with TUS (dabetic+TUS). All mice were surgically induced unilateral limb ischemia. The ischemic skeletal muscles in groups B and D were irradiated with extracorporeal TUS for 9 minutes/day (frequency of 1 MHz, intensity of 0.3 W/cm$^2$) for 14 consecutive days. The result showed that TUS augmented the blood perfusion, increased capillary density accompanied by an upregulation of angiogenic factors and a downregulation of apoptotic proteins in group D relative to group C. *In vitro*, TUS inhibited the apoptosis, promoted tubule formation, proliferation and migration capacities, increased angiogenic factors expression and reduced apoptotic protein levels in human umbilical vein endothelial cells (HUVECs). Furthermore, TUS can robust reverse the inhibiting effect induced by high glucose (HG) on HUVECs, and these benefits could be blocked by phosphoinositide 3-kinase (PI3K) inhibitor (LY294002) or eNOS inhibitor (L-NAME). Together, TUS restored type-2 DM-mediated inhibition of ischemia-induced angiogenesis, partially via PI3K-Akt-eNOS signal pathway.

**Keywords:** Angiogenesis, diabetic mice, hindlimb ischemia, therapeutic ultrasound

## Introduction

Progression of atherosclerosis leads to limb arteries occlusion and blood perfusion decline, known as peripheral artery disease (PAD) [1]. Type 2 diabetic Patients are frequently accompanied by PAD, and the morbidity of PAD in diabetic patients is 2-4 times higher than that in general population [2]. Therapeutic angiogenesis is a promising therapeutic strategy for ischemic episodes, including PAD. Although several agents or modalities have been demonstrated effective in healthy animals, the clinical efficacy and safety for facilitating angiogenesis during PAD are frustrating, one of the possible reasons may be lack of strict assessment in stable and cross-sectional animal models of clinical disease [3]. Thus, it is necessary to identify effective therapeutic strategies to stimulate ischemic-induced angiogenesis.

Ultrasound (US) is a physical wave form, and the frequency is higher than 20 kHz [4]. US has been universally employed in medical practice, including ultrasonography, tumor ablation, and tissue regeneration [5]. Recently, pro-angiogenic effects of low-intensity ultrasound have been confirmed in endothelial cells [6], a porcine

model of chronic ischemic heart disease (IHD) [4], and a mouse hindlimb ischemic model [7]. However, it is little known that the effect of low intensity TUS treatment on ischemic-induced angiogenesis in diabetic individuals.

In the current investigation, we introduced TUS to a HFD/STZ induced type-2 DM mouse model with hindlimb ischemia, and detected the protective effects of TUS in diabetes with PAD.

## Materials and methods

### *Animals*

4-week-old male C57BL/6 mice were housed in an environmentally controlled breeding room and allowed to have food and water freely. All animal operative protocols and procedures were approved by the Shanghai Jiao Tong University Animal Care and Use Committee.

### *Generation of diabetic mice*

The mouse model of type 2 diabetic was induced as described previously [8]. Briefly, the mice were allowed to have either a common mouse chow or a HFD, with a fat calories of 10% or 60%, respectively. 8 weeks later and after an overnight fasting, the mice were injected with either freshly prepared solution of STZ (100 mg/kg, i.p.) or vehicle (0.1 M citrate buffer, pH 4.5). Then all the mice were raised with their originally diets until sacrifice. 14 days after STZ injection, the HFD/STZ-induced mice displayed type 2 diabetes-like characteristic as previously described [9], such as hyperglycemia and insulin resistance (IR), the mice were accepted as successful type 2 diabetic mice.

### *Collection of blood and assay*

Blood glucose levels of mice were acquired by tail-vein blood glucose measurement with One Touch Ultra Glucometer (Johnson & Johnson, New Jersey, USA). Blood samples for total cholesterol (TC), triglyceride (TG), high density lipoprotein (HDL), low density lipoprotein (LDL), and insulin (INS) were collected from the retroorbital vein plexus. Fasting serum insulin (FINS) were detected by using an insulin ELISA kit (ALPCO Diagnostics, Windham, NH), while TC, TG, HDL and LDL were detected using an enzymatic colorimetric assay via an automatic biochemical analyzer. The homeostatic model assessment of insulin resistance (HOMA-IR) = FINS × FBG/22.5 [10].

### *Ischemic hindlimb model*

The mouse model of hindlimb ischemia was generated as previously described [11, 12]. All mice were anesthetized (40 mg/kg chloral hydrate, i.p.), and the left femoral artery between the inguinal ligament proximally and the popliteal fossa distally was surgically excised. The standard chow-fed mice and diabetic mice were randomly allocated to 4 groups: Control, Control+TUS, Diabetic, Diabetic+TUS.

### *TUS treatment*

Ultrasonic generator was made by Institute of Acoustics of Tongji University. TUS at frequency of 1.0 MHz and a density of 0.3 W/cm$^2$ was delivered by a cylindrically focused transducer with 2-cm diameter. The ischemic tissues of the mice were treated with active TUS or inactive TUS for 9 minutes/day in TUS or non-TUS groups, respectively. The treatment lasts for a continuous 14 days after surgery.

### *Necrosis score*

Assessment of hindlimb necrosis score was performed as previously described [7]. Briefly, on day 14 after surgery, the mice were scored in accordance with following standards: 0, necrosis or ulcer was not existed; 1, necrosis or ulcer can be detected; 2, amputation occurred under ankle; 3, amputation happened above ankle.

### *Thermal infrared imaging (TIRI) analysis*

The TIRI analyzer (Prism-DS 50137, FLIR Systems) were employed to measure the skin temperatures of both hindlimbs, and the color-coded images represented changes of blood flow. Dark-to-purple colors represented low skin temperature, and red-to-white colors expressed high skin temperature. At day 0 and day 14, TIRI measurements were performed, and perfusion data were reported from histograms of the colored pixels. To reduce the effects of ambient light, the ischemic/nonischemic limb temperature ratio were used to represent blood perfusion.

### *Immunofluorescence analysis*

Capillary density in each cross-section (5 μm) was labeled by immunofluorescence staining as previously reported [7, 13]. Briefly, after procedures of antigen retrieval and blocking, incu-

**Table 1.** Effect of TUS on physiological parameters in Control and Diabetic mice

| Parameters | Control | Control+TUS | Diabetic | Diabetic+TUS |
|---|---|---|---|---|
| BW (g) | 28.23±0.95 | 27.41±0.80 | 32.88±0.96** | 32.55±0.87 |
| TC (mmol/L) | 2.61±0.11 | 2.36±0.08 | 3.92±0.11** | 3.73±0.19 |
| TG (mmol/L) | 1.10±0.06 | 1.07±0.07 | 1.39±0.14 | 1.40±0.11 |
| HDL (mmol/L) | 2.08±0.04 | 1.98±0.03 | 3.56±0.06** | 3.34±0.12 |
| LDL (mmol/L) | 0.32±0.02 | 0.30±0.02 | 0.61±0.04** | 0.54±0.05 |
| FBG (mmol/L) | 5.43±0.26 | 5.07±0.23 | 17.83±1.20** | 17.20±1.33 |
| FINS (mIU/L) | 10.52±0.70 | 10.36±0.54 | 19.59±0.67** | 19.47±0.66 |
| HOMA-IR | 2.57±0.27 | 2.32±0.12 | 15.62±1.45** | 14.75±0.95 |

Values report mean ± SEM, n = 6. $^{**}P < 0.01$ vs. Control.

bation with goat anti-CD31 antibody (BD, Franklin Lakes, NJ) and secondary antibody (Invitrogen, Carlsbad, CA, USA) were successively performed. 10 random microscopic fields (× 320 magnification) in each mouse were counted, and the density of capillary was determined as the number of capillaries/field.

*Western blotting analysis*

Protein contents in ischemic muscles and HUVECs were detected by Western blot as described previously [13]. Briefly, equal amounts of tissue/cell proteins were dissociated, homogenized, electrotransferred, and immunoblotted with anti-eNOS, anti-Akt, anti-p-Akt (Ser473), anti-bcl-2, anti-bax, anti-caspas3, anti-cleaved-caspas3 (Cell Signaling Technology, Danvers, MA, USA), anti-vascular endothelial growth factor (VEGF) (Beyotime, Haimen, China) and anti-β-actin (Sigma, St. Louis, MO, USA). Interested genes were captured with a FluorChem E data system (Cell Biosciences, Santa Clara, CA) and the densitometry was analyzed by ImageJ software. Containing β-actin levels were used as an internal control to normalize the data.

*Cell culture*

HUVECs (ATCC, Cat. CRL1730) were incubated as previously described [14]. Cells ($1 \times 10^5$ per 75-$cm^2$-flask) were cultivated in DMEM medium (low-glucose) added with 100 U/ml penicillin and 100 U/ml streptomycin, together with 10 percent fetal bovine serum. The incubations were kept at 37°C, 5% $CO_2$ and 95% air. In experiments, passages 3-5 HUVECs were used. HUVECs were grouped into 6 experimental groups: normal glucose (Control, 5 mM glucose), normal glucose plus TUS (9 min/day for 3 consecutive days, 1 MHz, 0.3 W/$cm^2$), high glucose (HG, 33 mM glucose), high glucose plus TUS (9 min/day for 3 consecutive days, 1 MHz, 0.3 W/$cm^2$), LY294002 (20 μM) and high glucose plus TUS (9 min/day for 3 consecutive days, 1 MHz, 0.3 W/$cm^2$), L-NAME (100 μM) and high glucose plus TUS (9 min/day for 3 consecutive days, 1 MHz, 0.3 W/$cm^2$). 72 hours later, cells were harvested for biological analysis, including proliferation, migration, tubule formation, apoptosis and immunoblotting assay.

*CCK-8 assay*

WST-8 Cell Counting Kit-8 (CCK-8 kit; Beyotime, Haimen, China) was adopted to analyze cells proliferation. Briefly, pretreated cells were collected and reseeded into 96-well plates ($2 \times 10^3$ cells/100 μL/well), and culture plates were exposed to their original mediators for 24 h. Cells were then kept at 37°C for 2 h after adding CCK-8 solution (10 μL/well). The final reaction system absorbance was captured at 450 nm wavelength.

*Evaluation of cell apoptosis*

After 72 hours incubation, apoptosis was examined by Hoechst staining (Beyotime, Haimen, China) according to the instruction of its manufacturer. The apoptotic ratio was represented as (positive staining cell numbers)/(total cells) × 100%.

*Matrigel tubule formation assay*

Pretreated HUVECs ($2.5 \times 10^4$/well) were reseeded into Matrigel (BD Biosciences, Bedford, MA) coated 96-well dishes, and exposed to their original mediators for 8 h. Graphs were captured with a fluorescent microscope (IX-71; Olympus) equipped with 12.8 M pixel recording digital color cooled camera (DP72; Olympus). Tubule formation was represented as fold of control.

*Transwell migration assay*

24-well Boyden Transwell chambers (Corning, Cambridge, MA) were employed to determine cells migration. In brief, original incubation

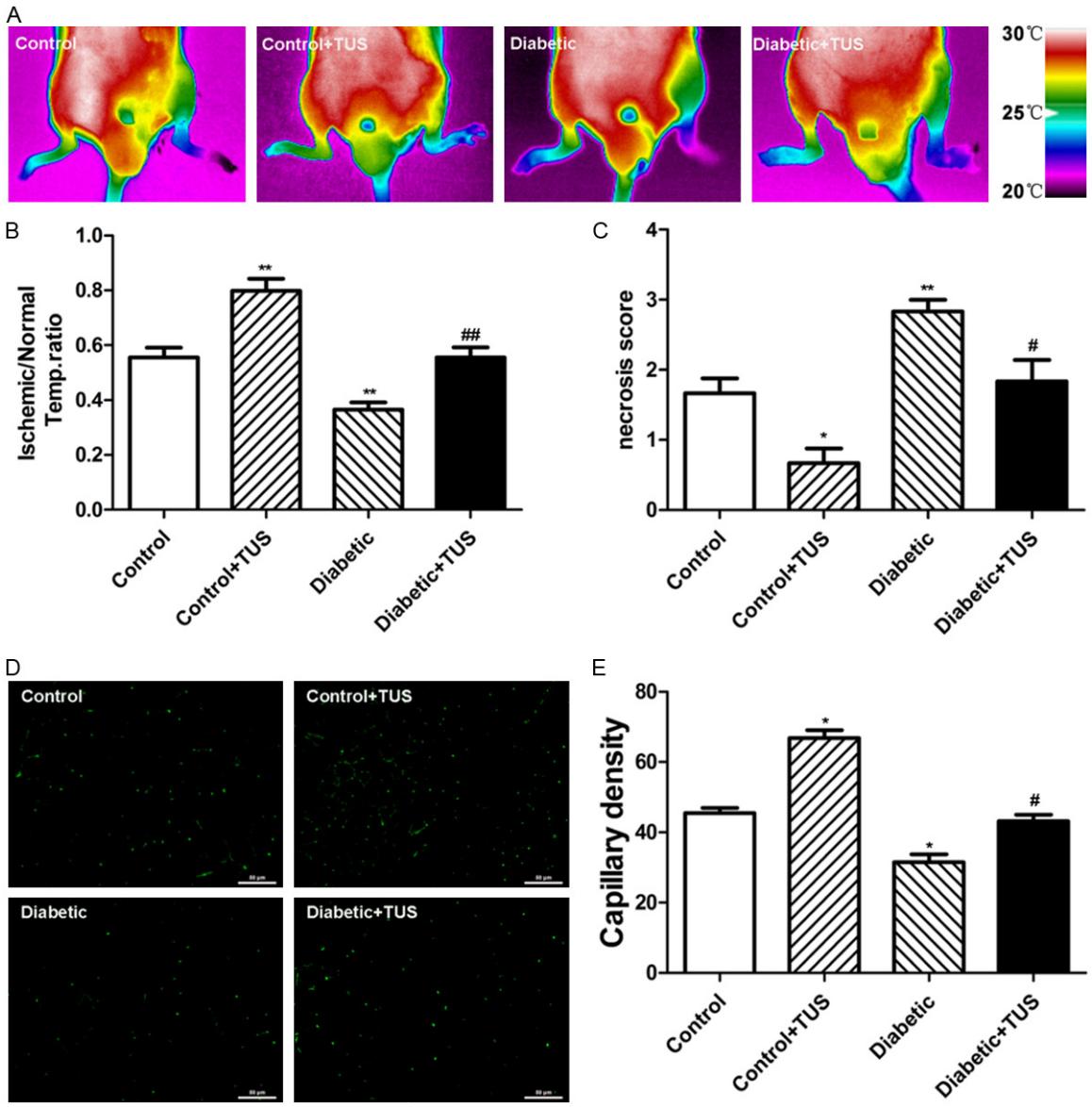


**Figure 1.** TUS effects on the blood flow of the ischemic hindlimb in diabetic mice. A. Representative infrared spectrum imaging of hindlimb on day 14 after the induction of ischemia. B. Infrared thermal imaging data was quantitated and depicted as an ischemic/non-ischemic hindlimb temperature ratio. C. Necrosis score was evaluated in terms of a recognized evaluation standard on day 14. D. Representative images of immunofluorescence staining with an anti-CD31 of 4 groups (magnification × 320, Scale bar = 50 μm). E. Quantification analysis of capillary density (capillaries/field) in 4 individual groups of mice. Values were shown as mean ± SEM, n = 6. $^{*}P < 0.05$ vs. Control. $^{**}P < 0.01$ vs. Control. $^{\#}P < 0.05$ vs. Diabetic. $^{\#\#}P < 0.01$ vs. Diabetic.

mediators (600 μL) were added to lower chambers, corresponding pretreated HUVECs (2 × $10^4$/well/100 μL) were reseeded in upper chambers in serum-free Medium. 8 hours later, migrated HUVECs were counted with light microscopy (× 100 magnification).

*Statistical analysis*

Data were expressed as mean ± SEM. Statistical significance was analyzed by One-way analysis of variance (ANOVA) followed by Tukey's post-hoc test. *P* Values < 0.05 were accepted significance.

## Results

*Physiological parameters*

The BW, FBG, HOMA-IR, FINS, LDL, HDL, TC and TG of the Control group, Control+TUS group, Diabetic group and Diabetic+TUS group are

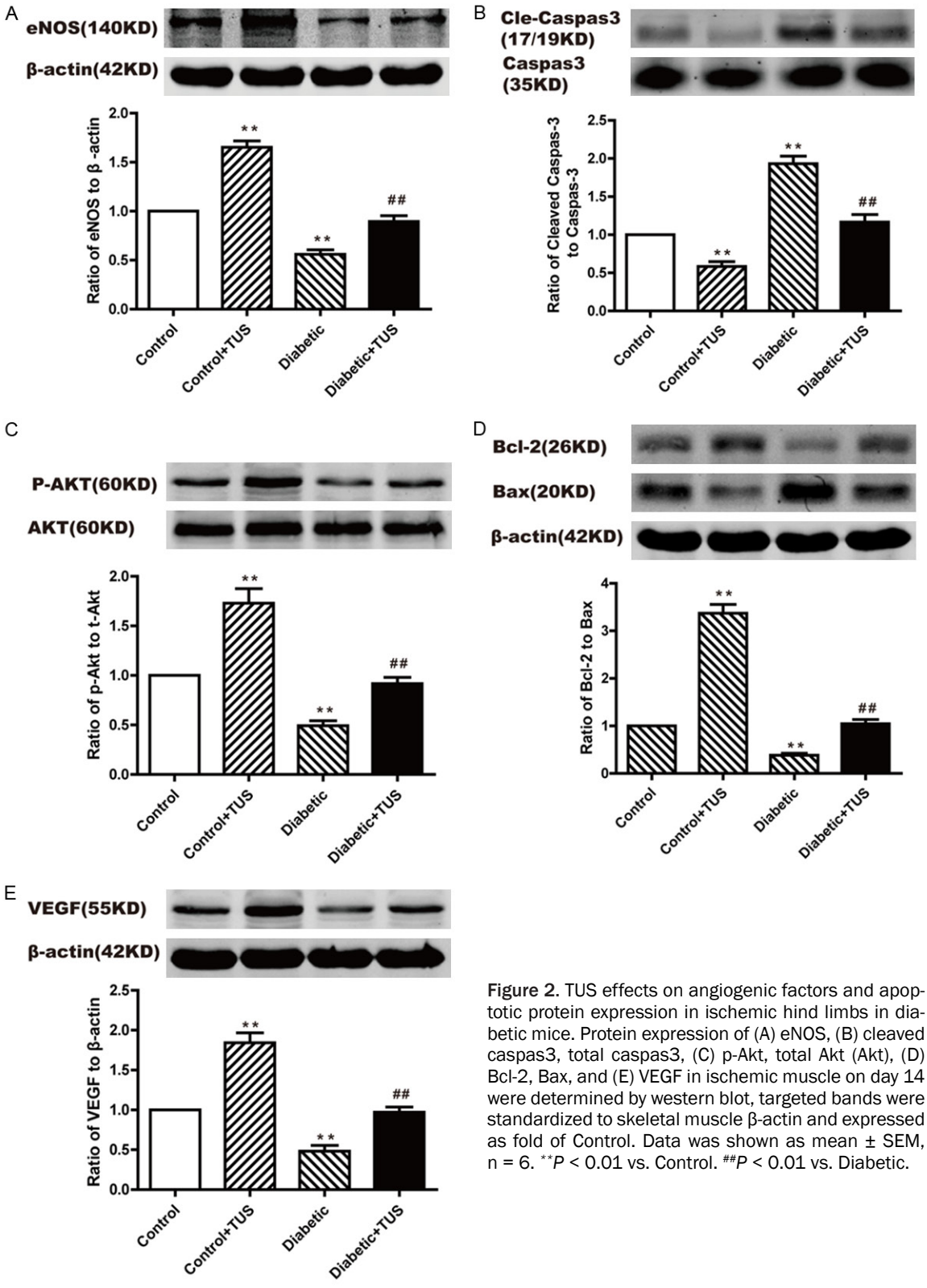


**Figure 2.** TUS effects on angiogenic factors and apoptotic protein expression in ischemic hind limbs in diabetic mice. Protein expression of (A) eNOS, (B) cleaved caspas3, total caspas3, (C) p-Akt, total Akt (Akt), (D) Bcl-2, Bax, and (E) VEGF in ischemic muscle on day 14 were determined by western blot, targeted bands were standardized to skeletal muscle β-actin and expressed as fold of Control. Data was shown as mean ± SEM, n = 6. $^{**}P < 0.01$ vs. Control. $^{\#\#}P < 0.01$ vs. Diabetic.

summarized in **Table 1**. Although, all the parameters in Diabetic group and Diabetic+TUS group are higher than that in Control counterparts, there were no statistical differences of all items in Control+TUS and Diabetic+TUS groups relative to their untreated groups.

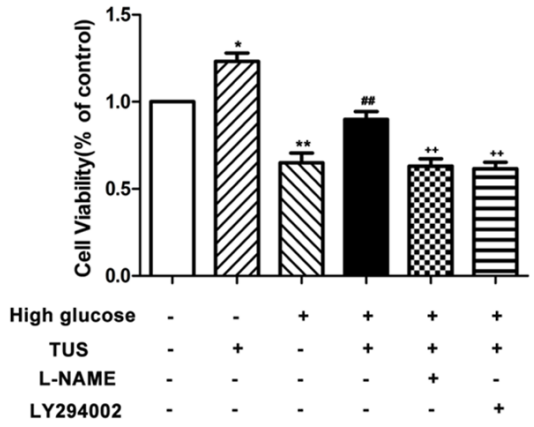


**Figure 3.** Proliferation effects of TUS on HUVECs. HUVECs were treated with 6 different mediators for 24 h. Viability of HUVECs was measured by Cell Count Kit-8 (CCK-8). Data was reported as mean ± SEM, n = 3. $^{*}P < 0.05$ vs. Control. $^{**}P < 0.01$ vs. Control. $^{\#\#}P < 0.01$ vs. HG. $^{++}P < 0.01$ vs. HG+TUS.

*TUS increases hindlimb blood perfusion and vascular density in the diabetic mouse model*

Hyperglycemia is a leading hazard factor for the progression of PAD, which is closely related to type 2 diabetes [15]. To investigate whether TUS treatment would be conducive to tissue restoration, we evaluated the hindlimb ischemic scores on day 14 after surgery in a diabetic mouse model with PAD. As expected, the ischemic scores of non-treated mice were obviously higher than TUS treated ones either in Control groups or diabetic groups, indicating that TUS can signally accelerate wound healing after ischemic attack (**Figure 1C**).

By using the apparatus of TIRI, blood flow of all the mice were detected. On day 14 after surgery, the diabetic mice displayed a lower blood flow ratio than Control mice, and TUS can augment blood perfusion in Control+TUS mice and normalize it in diabetic+TUS group (**Figure 1A** and **1B**). These data demonstrated that TUS treatment is efficient in recovering blood flow in the diabetic PAD model.

To deep illuminate the newborn capillaries facilitated blood perfusion, the capillary density of ischemic tissues was measured. Immunofluorescence staining showed that TUS augmented angiogenesis in TUS treated mice. Although, diabetic mice exhibited capillary rarefaction relative to controls, TUS treatment can dramatically restore the inhibiting effect in diabetic group and augment the density in Control+TUS group (**Figure 1D** and **1E**).

*TUS treatment improves angiogenic factors and inhibits apoptosis responses in the diabetic model*

To illuminate the underlying molecular mechanisms of the TUS-induced tissue recovery in diabetic mice, the angiogenic factors of eNOS, VEGF, p-Akt, antiapoptotic factors of bcl-2 and apoptotic factors of bax, cleaved caspas3 in ischemic tissues were detected. When compared with Control group, TUS upregulated angiogenic factors, antiapoptotic factors and downregulated apoptotic factors in Control+TUS group. In contrast, angiogenic, antiapoptotic proteins were suppressed and apopotic factors were activated in diabetic mice compared with control ones, but these changes were restored in diabetic+TUS group by TUS treatment (**Figure 2**). These results manifested that angiogenic factors and antiapoptotic proteins could act synergistically for appropriate vascular growth, and TUS treatment could strongly improve these effects.

*TUS facilitated the HUVECs proliferation*

To survey the role of TUS on endothelial proliferation, HUVECs were incubated for 24 h and analyzed by CCK-8 assay. The numbers of HUVECs were lower in HG than in Control. Interestingly, TUS was able to enhance the proliferation of HUVECs in HG+TUS in comparison with that in HG. In addition, TUS treatment also increased the number of HUVECs in Control+TUS when compared with Control group. However, L-NAME or LY294002 can eliminate the promoting effect of TUS (**Figure 3**).

*TUS augmented tube formation*

Previous study has shown that TUS can improve the tubule formation of HUVECs in normal media [14]. However, it is little known whether TUS influences tubule formation under HG media. As is depicted in the picture (**Figure 4**), tubule length in high glucose media was significantly lower compared with that in normal glucose media. It is noteworthy that not only TUS enhanced tubule length in Control+TUS, but also restored tubule length in HG+TUS relative to control. However, this protective effect of TUS could be abrogated by pre-incubation of L-NAME or LY294002.

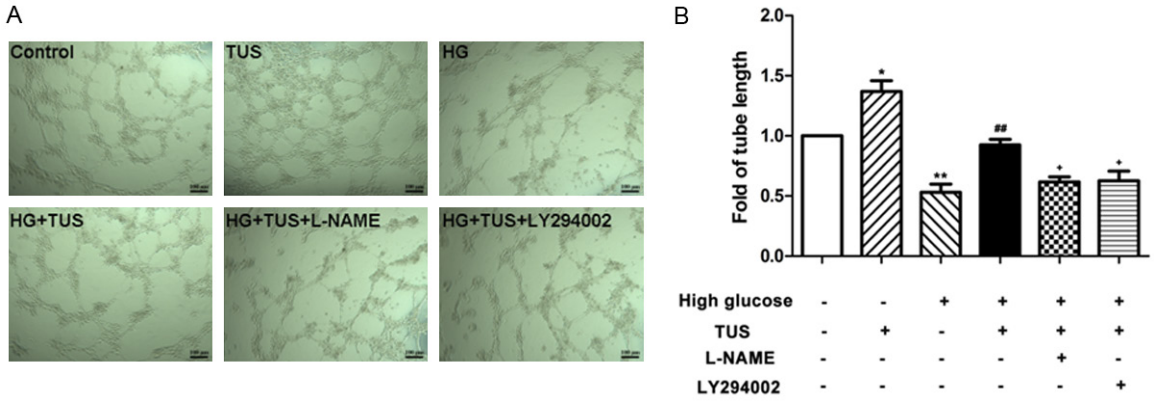


**Figure 4.** TUS increased tubule formation induced by HG in HUVECs. HUVECs were exposed to 6 different mediators and treatment for 8 h. A. Representative images of tube formation in cultured HUVECs. B. Quantitative analysis of tube length was represented as fold of control (× 100 magnification), Data was reported as mean ± SEM, n = 3. $^{*}P < 0.05$ vs. Control. $^{**}P < 0.01$ vs. Control. $^{\#\#}P < 0.01$ vs. HG. $^{+}P < 0.05$ vs. HG+TUS. Scale bar = 100 μm.

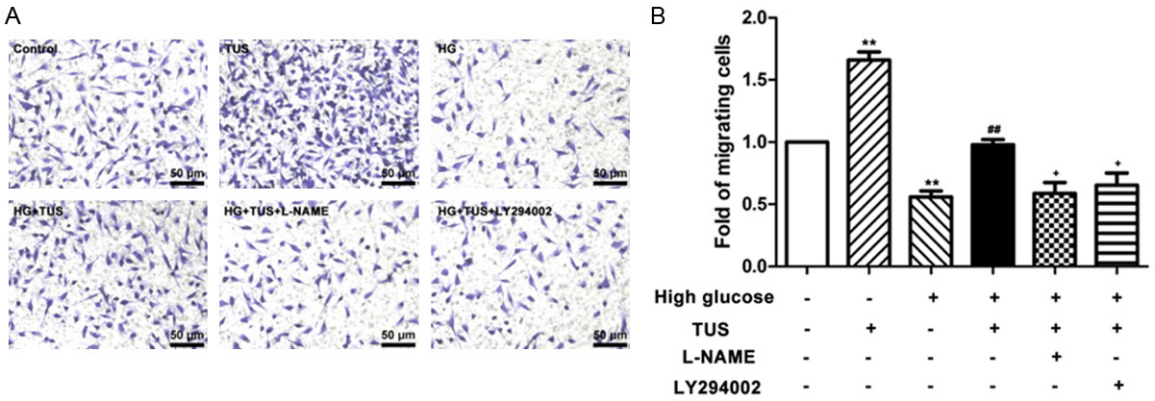


**Figure 5.** TUS promotes the migration induced by HG in HUVECs. HUVECs were incubated with 6 different mediators for 8 h. A. Migrated cells were stained. B. Quantitative analysis of migrated cells was shown as fold of control (× 100 magnification), Data was reported as mean ± SEM, n = 3. $^{**}P < 0.01$ vs. Control. $^{\#\#}P < 0.01$ vs. HG. $^{+}P < 0.05$ vs. HG+TUS. Scale bar = 50 μm.

*TUS enhances migration in vitro*

The numbers of migrated HUVECs cultured with HG were strikingly lower than that from Control, and this suppression could be restored by TUS in HG+TUS group. This protective effect was observed in Control+TUS group as well. As expected, these benefits could be blocked by L-NAME or LY294002 (**Figure 5**).

*TUS inhibits HG-induced HUVEC apoptosis*

Hoechst staining was employed to examine HG-induced HUVECs apoptosis, compared with normal glucose culture, HG prominently accelerated the apoptotic cell numbers, TUS could markedly promote cell survival in normal glucose culture and dramatically attenuate HG-induced apoptosis. However, L-NAME or LY294002 pretreatment abrogated TUS anti-apoptotic effect (**Figure 6**).

*TUS enhanced angiogenic factors and suppressed apoptotic responses in vitro*

When compared with Control group, TUS increased angiogenic factors (eNOS, VEGF, p-Akt and bcl-2) and downregulated apoptotic proteins (bax and cleaved caspas3) in Control+TUS group. In contrast, HG incubation exhibited lower angiogenesis proteins and higher apoptosis factors relative to normal glucose, but this situation was corrected in HG+TUS group by TUS treatment. Interestingly, the profits of TUS can be eliminated by administration of L-NAME or LY294002 (**Figure 7**).

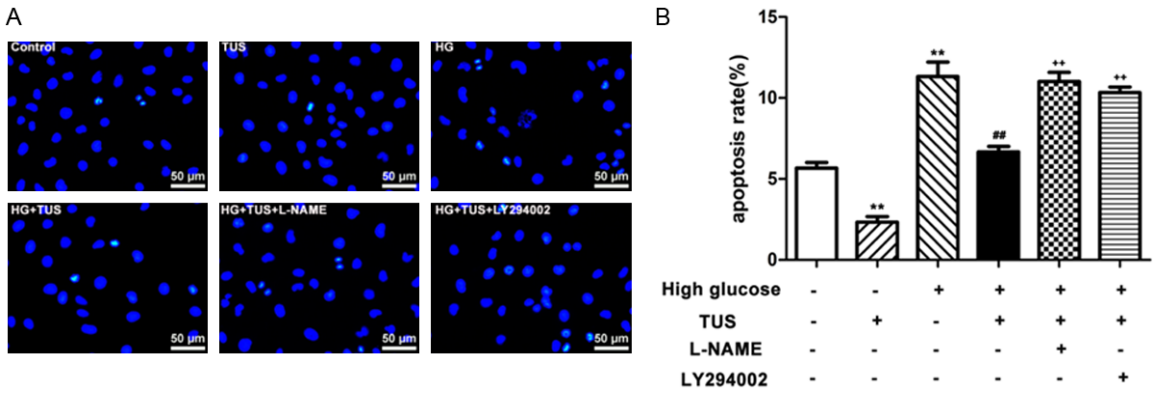


**Figure 6.** TUS reduces cell apoptosis induced by HG in HUVECs. HUVECs were incubated with different mediators for 72 h. A. Representative photomicrographs of Hoechst Staining in cultured HUVECs. B. Data was represented as the apoptotic cells in the total cells per field. Values were expressed as mean ± SEM, n = 3. **P < 0.01 vs. Control. ##P < 0.01 vs. HG. ++P < 0.01 vs. HG+TUS. Scale bar indicated 50 μm.

## Discussion

In the current investigation, we manifested that TUS induced revascularization in the ischemic muscles in hyperglycemia setting through activating angiogenic pathways and downregulating apoptotic pathways, and the protective effects of TUS work via a PI3K-Akt-eNOS dependent manner.

Hyperglycemia or HG microenvironment mediated endothelial dysfunction and apoptosis are significant in diabetes-related cardiovascular complications, including retarded angiogenesis and accelerated apoptosis [16, 17]. Several possible mechanisms should take responsibility for retarded angiogenesis in the diabetic setting: 1), HG-related endothelial dysfunction and inhibition of eNOS activity may account for the impaired angiogenic response. Previous study showed that long-term exposure to HG suppressed the activity of eNOS in incubated HUVECs [16], and angiogenic response after tissue ischemia exhibited rarefaction in eNOS-deficient mice [18]. 2), Overwhelming reactive oxygen species (ROS) induced by HG exacerbated cellular toxicity, triggered endothelial dysfunction and apoptosis. Apoptosis of endothelial cells (ECs) may badly hamper the endothelial monolayer integrity and damage vascular wall, resulting in the loss of microvessels [19]. 3), HG itself might directly disturb ECs activities. Altogether, endothelial dysfunction and superfluous ROS should responsible to impaired angiogenesis in the HG microenvironment.

The underlying mechanisms of hindlimb ischemic injury remain elusive. However, inhibition of ECs apoptosis and promotion of angiogenesis could minimize hindlimb ischemia [20, 21]. Akt, a downstream molecule of PI3K, is a multifunctional conditioner of cell survival, apoptosis, angiogenesis, and protein synthesis [22]. Activating PI3K-Akt-eNOS signal pathway can promote cell survival [23]. Over-expression of VEGF level can lessen or abrogate hindlimb ischemia by promoting new vessels formation, which is known as therapeutic angiogenesis [24]. The Bcl-2 family proteins are strong manipulators of apoptosis, including two families: pro-apoptotic factors such as Bax and anti-apoptotic factors such as Bcl-2. The extent of apoptosis is often expressed as Bcl-2/Bax ratio [25]. Caspase-3, a main element of the proteolytic cascade, acts as a significant role in the cell apoptosis process [26].

TUS can produce multitudinous biological effects *in vitro* and *in vivo*. Investigations revealed that application of ultrasound can augment angiogenic cells growth and migration abilities [27], enhance perfusion and capillary numbers of rats undergoing hindlimb ischemic attack [28]. In addition to proangiogenesis, numerous investigations have shown that US can exert anti-inflammatory effects, anti-oxidant responses and antiapoptotic effects [29-31]. Consistent with previous investigations, our work confirmed that TUS significantly reversed ischemia-mediated angiogenesis (increased blood flow and capillary density) in the HFD/STZ induced diabetic mouse model. These beneficial effects were also affirmed in the normoglycemic mice.

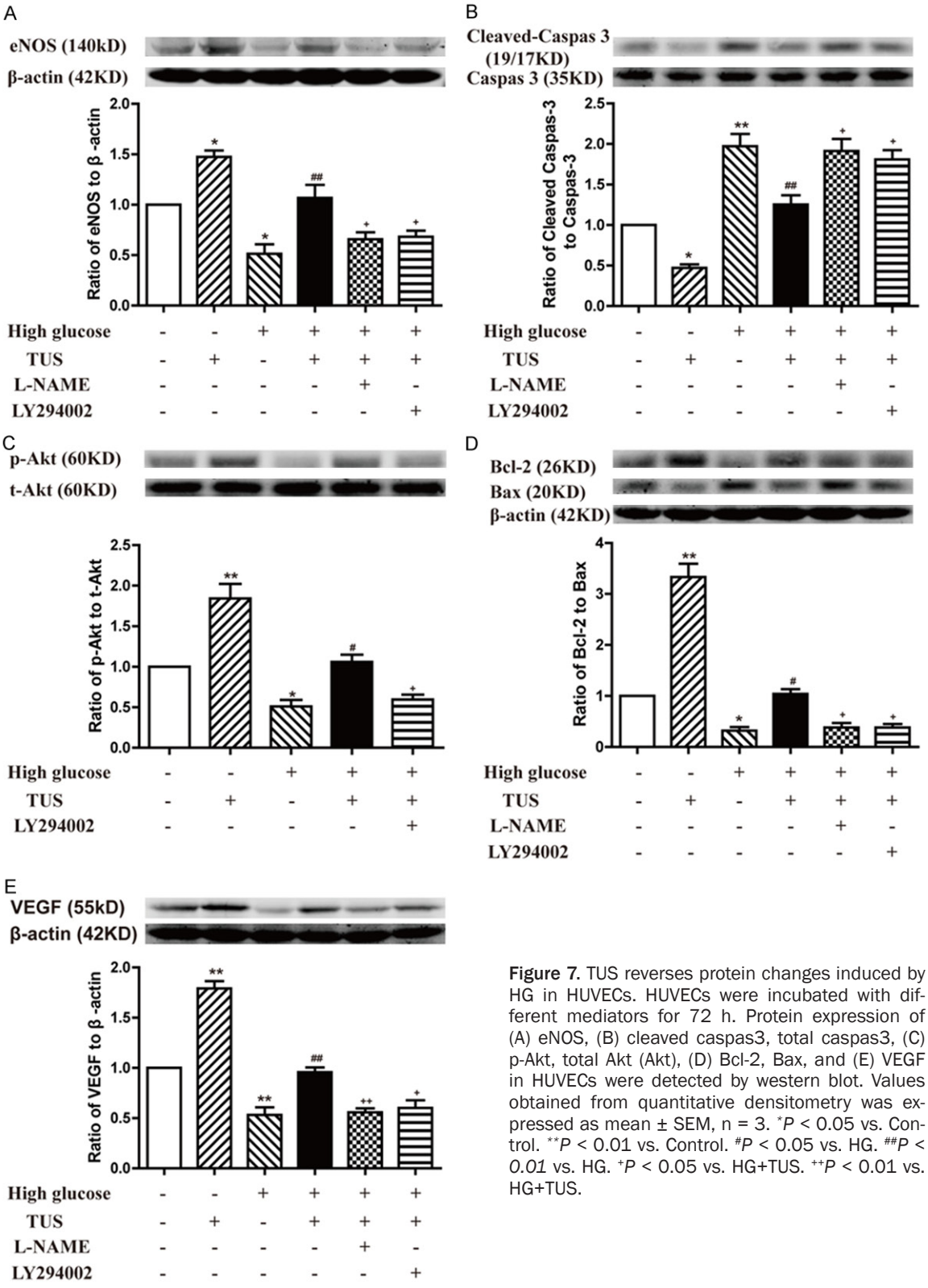


**Figure 7.** TUS reverses protein changes induced by HG in HUVECs. HUVECs were incubated with different mediators for 72 h. Protein expression of (A) eNOS, (B) cleaved caspas3, total caspas3, (C) p-Akt, total Akt (Akt), (D) Bcl-2, Bax, and (E) VEGF in HUVECs were detected by western blot. Values obtained from quantitative densitometry was expressed as mean ± SEM, n = 3. $^{*}P < 0.05$ vs. Control. $^{**}P < 0.01$ vs. Control. $^{\#}P < 0.05$ vs. HG. $^{\#\#}P < 0.01$ vs. HG. $^{+}P < 0.05$ vs. HG+TUS. $^{++}P < 0.01$ vs. HG+TUS.

And these beneficial effects were associated with increased angiogenic factors of eNOS, VEGF, p-Akt and bcl-2 as well as reduced apoptotic factors of bax and cleaved caspas3 in ischemic muscles. It could be summarized that improved angiogenesis and suppressed apop-

tosis by TUS might be in part through PI3K-Akt-eNOS pathway. It is noteworthy that the beneficial effects of TUS were not due to changes of blood lipid, blood glucose, or plasma insulin, since there were no statistical differences between TUS treated group and non-TUS group, while these indexes were dramatically higher in diabetic mice compared to normal ones.

To better illuminate the mechanism by which TUS succeeded in augmenting angiogenesis and inhibiting apoptosis in diabetic mice, we investigated TUS-induced endothelial functional *in vitro*. Results showed that TUS can augment multiple endothelial functions including reduced apoptotic cells, enhanced activity of tube formation, increased cell proliferation and migration, together with improved angiogenic factors, antiapoptosis proteins and reduced apoptotic factors. Previous study revealed that the PI3K-Akt pathway was damaged in type 2 diabetic mice [32], and eNOS activity was impaired in diabetic mice and in episode of endothelial dysfunction [33]. However, TUS can significantly upregulate eNOS activity [14]. Based on foregoing clues, we investigated the role of PI3K-Akt-eNOS pathway in TUS-induced agiogenesis. Results indicated that TUS-induced endothelial protective effects in response to HG can be abrogated by LY294002 or L-NAME. Altogether, these data fully demonstrated that TUS performs its proangiogenic and antiapoptotic effects via the PI3K-Akt-eNOS pathway.

In summary, the current investigation indicates that TUS eliminates HG/hyperglycemia mediated ECs dysfunction in both *in vivo* and *in vitro* via PI3K-Akt-eNOS pathway. It can repair blood reperfusion, decrease necrosis and promote angiogenesis in a diabetic with PAD model. Our results indicate that TUS treatment for diabetic PAD may represent a useful clinical approach to advance angiogenesis and rescue tissue ischemia.

## Acknowledgements

This work was supported by the China National Natural Science Foundation (11574210, 1137-4213, 81500372 and 81500523), Shanghai Pujiang Program (15PJ1405000) and Foundation of National Lab for Infrared Physics (200901).

## Disclosure of conflict of interest

None.

**Address correspondence to:** Dr. Jun-Li Duan, Department of Gerontology, Xinhua Hospital, Shanghai Jiaotong University, Kongjiang Road 1665, Shanghai 200092, China. Tel: +86-21-25071115; Fax: +86-21-65795173; E-mail: duanjunlixh@163.com; Dr. Chang-Ning Hao, Ren Ji Hospital, Shanghai Jiaotong University School of Medicine, Dongfang Road 1630, Shanghai 200127, China. Tel: +86-21-2507-7715; Fax: +86-21-6549-3951; E-mail: gilberthaocn@gmail.com; Dr. Yi-Qin Shi, Department of Nephrology Zhongshan Hospital, Fudan University, Fenglin Road 180, Shanghai 200032, China. Tel: +86-21-64041990; Fax: +86-21-64041990; E-mail: jennyshiyiqin@gmail.com; Dr. Yue Li, Department of Internal Medicine, University of Iowa Carve College of Medicine 2000 Medical Laboratories, 25 South Grand Avenue, Iowa City, IA 52242, USA. Tel: +1-319-384-1187; E-mail: yue-li-2@uiowa.edu

## References

[1] Iwabayashi M, Taniyama Y, Sanada F, Azuma J, Iekushi K, Kusunoki H, Chatterjee A, Okayama K, Rakugi H and Morishita R. Role of serotonin in angiogenesis: induction of angiogenesis by sarpogrelate via endothelial 5-HT1B/Akt/eNOS pathway in diabetic mice. Atherosclerosis 2012; 220: 337-342.

[2] Mukherjee D. Peripheral and cerebrovascular atherosclerotic disease in diabetes mellitus. Best Pract Res Clin Endocrinol Metab 2009; 23: 335-345.

[3] Higashi Y, Nishioka K, Umemura T, Chayama K and Yoshizumi M. Oxidative stress, endothelial function and angiogenesis induced by cell therapy and gene therapy. Curr Pharm Biotechnol 2006; 7: 109-116.

[4] Hanawa K, Ito K, Aizawa K, Shindo T, Nishimiya K, Hasebe Y, Tuburaya R, Hasegawa H, Yasuda S, Kanai H and Shimokawa H. Low-intensity pulsed ultrasound induces angiogenesis and ameliorates left ventricular dysfunction in a porcine model of chronic myocardial ischemia. PLoS One 2014; 9: e104863.

[5] ter Haar G. Therapeutic applications of ultrasound. Prog Biophys Mol Biol 2007; 93: 111-129.

[6] Cao WJ, Rosenblat JD, Roth NC, Kuliszewski MA, Matkar PN, Rudenko D, Liao C, Lee PJ and Leong-Poi H. Therapeutic Angiogenesis by Ultrasound-Mediated MicroRNA-126-3p Delivery. Arterioscler Thromb Vasc Biol 2015; 35: 2401-2411.

[7] Huang JJ, Shi YQ, Li RL, Hu A, Zhou HS, Cheng Q, Xu Z, Yang ZM, Hao CN and Duan JL. Angiogenesis effect of therapeutic ultrasound on ischemic hind limb in mice. Am J Transl Res 2014; 6: 703-713.

[8] Luo J, Quan J, Tsai J, Hobensack CK, Sullivan C, Hector R and Reaven GM. Nongenetic mouse models of non-insulin-dependent diabetes mellitus. Metabolism 1998; 47: 663-668.

[9] DeFronzo RA. Pharmacologic therapy for type 2 diabetes mellitus. Ann Intern Med 1999; 131: 281-303.

[10] Lee S, Muniyappa R, Yan X, Chen H, Yue LQ, Hong EG, Kim JK and Quon MJ. Comparison between surrogate indexes of insulin sensitivity and resistance and hyperinsulinemic euglycemic clamp estimates in mice. Am J Physiol Endocrinol Metab 2008; 294: E261-270.

[11] Hao C, Huang ZH, Song SW, Shi YQ, Cheng XW, Murohara T, Lu W, Su DF and Duan JL. Arterial baroreflex dysfunction impairs ischemia-induced angiogenesis. J Am Heart Assoc 2014; 3: e000804.

[12] Hao C, Shintani S, Shimizu Y, Kondo K, Ishii M, Wu H and Murohara T. Therapeutic angiogenesis by autologous adipose-derived regenerative cells: comparison with bone marrow mononuclear cells. Am J Physiol Heart Circ Physiol 2014; 307: H869-879.

[13] Li RL, Huang JJ, Shi YQ, Hu A, Lu ZY, Weng L, Wang SQ, Han YP, Zhang L, Hao CN and Duan JL. Pulsed electromagnetic field improves postnatal neovascularization in response to hindlimb ischemia. Am J Transl Res 2015; 7: 430-444.

[14] Huang JJ, Shi YQ, Li RL, Hu A, Lu ZY, Weng L, Wang SQ, Han YP, Zhang L, Li B, Hao CN and Duan JL. Angiogenesis effect of therapeutic ultrasound on HUVECs through activation of the PI3K-Akt-eNOS signal pathway. Am J Transl Res 2015; 7: 1106-1115.

[15] Jude EB, Eleftheriadou I and Tentolouris N. Peripheral arterial disease in diabetes--a review. Diabet Med 2010; 27: 4-14.

[16] Ho FM, Lin WW, Chen BC, Chao CM, Yang CR, Lin LY, Lai CC, Liu SH and Liau CS. High glucose-induced apoptosis in human vascular endothelial cells is mediated through NF-kappaB and c-Jun NH2-terminal kinase pathway and prevented by PI3K/Akt/eNOS pathway. Cell Signal 2006; 18: 391-399.

[17] Sheikh AQ, Kuesel C, Taghian T, Hurley JR, Huang W, Wang Y, Hinton RB and Narmoneva DA. Angiogenic microenvironment augments impaired endothelial responses under diabetic conditions. Am J Physiol Cell Physiol 2014; 306: C768-778.

[18] Dai X and Faber JE. Endothelial nitric oxide synthase deficiency causes collateral vessel rarefaction and impairs activation of a cell cycle gene network during arteriogenesis. Circ Res 2010; 106: 1870-1881.

[19] Castela A and Costa C. Molecular mechanisms associated with diabetic endothelial-erectile dysfunction. Nat Rev Urol 2016; 13: 266-274.

[20] Cho SW, Hartle L, Son SM, Yang F, Goldberg M, Xu Q, Langer R and Anderson DG. Delivery of small interfering RNA for inhibition of endothelial cell apoptosis by hypoxia and serum deprivation. Biochem Biophys Res Commun 2008; 376: 158-163.

[21] Duan J, Murohara T, Ikeda H, Katoh A, Shintani S, Sasaki K, Kawata H, Yamamoto N and Imaizumi T. Hypercholesterolemia inhibits angiogenesis in response to hindlimb ischemia: nitric oxide-dependent mechanism. Circulation 2000; 102: III370-376.

[22] Liao Y and Hung MC. Physiological regulation of Akt activity and stability. Am J Transl Res 2010; 2: 19-42.

[23] Kim I, Kim HG, So JN, Kim JH, Kwak HJ and Koh GY. Angiopoietin-1 regulates endothelial cell survival through the phosphatidylinositol 3'-Kinase/Akt signal transduction pathway. Circ Res 2000; 86: 24-29.

[24] Fukuda S, Kaga S, Sasaki H, Zhan L, Zhu L, Otani H, Kalfin R, Das DK and Maulik N. Angiogenic signal triggered by ischemic stress induces myocardial repair in rat during chronic infarction. J Mol Cell Cardiol 2004; 36: 547-559.

[25] Levkau B, Schafers M, Wohlschlaeger J, von Wnuck Lipinski K, Keul P, Hermann S, Kawaguchi N, Kirchhof P, Fabritz L, Stypmann J, Stegger L, Flogel U, Schrader J, Fischer JW, Hsieh P, Ou YL, Mehrhof F, Tiemann K, Ghanem A, Matus M, Neumann J, Heusch G, Schmid KW, Conway EM and Baba HA. Survivin determines cardiac function by controlling total cardiomyocyte number. Circulation 2008; 117: 1583-1593.

[26] Wang X, Zelenski NG, Yang J, Sakai J, Brown MS and Goldstein JL. Cleavage of sterol regulatory element binding proteins (SREBPs) by CPP32 during apoptosis. EMBO J 1996; 15: 1012-1020.

[27] Toyama Y, Sasaki K, Tachibana K, Ueno T, Kajimoto H, Yokoyama S, Ohtsuka M, Koiwaya H, Nakayoshi T, Mitsutake Y, Chibana H, Itaya N and Imaizumi T. Ultrasound stimulation restores impaired neovascularization-related capacities of human circulating angiogenic cells. Cardiovasc Res 2012; 95: 448-459.

[28] Nazer B, Ghahghaie F, Kashima R, Khokhlova T, Perez C, Crum L, Matula T and Hata A. Therapeutic Ultrasound Promotes Reperfusion and Angiogenesis in a Rat Model of Peripheral Arterial Disease. Circ J 2015; 79: 2043-2049.

[29] Abe Y, Ito K, Hao K, Shindo T, Ogata T, Kagaya Y, Kurosawa R, Nishimiya K, Satoh K, Miyata S, Kawakami K and Shimokawa H. Extracorporeal low-energy shock-wave therapy exerts anti-inflammatory effects in a rat model of acute myocardial infarction. Circ J 2014; 78: 2915-2925.

[30] Martins CN, Moraes MB, Hauck M, Guerreiro LF, Rossato DD, Varela AS Jr, da Rosa CE and Signori LU. Effects of cryotherapy combined with therapeutic ultrasound on oxidative stress and tissue damage after musculoskeletal contusion in rats. Physiotherapy 2015; [Epub ahead of print].

[31] Zhang C, Teng F, Tu J and Zhang D. Ultrasound-enhanced protective effect of tetramethylpyrazine against cerebral ischemia/reperfusion injury. PLoS One 2014; 9: e113673.

[32] Kobayashi T, Taguchi K, Yasuhiro T, Matsumoto T and Kamata K. Impairment of PI3-K/Akt pathway underlies attenuated endothelial function in aorta of type 2 diabetic mouse model. Hypertension 2004; 44: 956-962.

[33] Tabit CE, Chung WB, Hamburg NM and Vita JA. Endothelial dysfunction in diabetes mellitus: molecular mechanisms and clinical implications. Rev Endocr Metab Disord 2010; 11: 61-74.